Journal of Veterinary Cardiology (2010) **12**, 111—121

ELSEVIER

Journal of Veterinary Cardiology
ESVC

www.elsevier.com/locate/jvc

Assessment of left ventricular size and function in horses using anatomical M-mode echocardiography

Patrizia A. Grenacher, med. vet. [a],
Colin C. Schwarzwald, Dr. med. vet., PhD [a,b,*]

[a] *Equine Department, Vetsuisse Faculty, University of Zurich, Winterthurerstrasse 260, 8057 Zurich, Switzerland*
[b] *Department of Veterinary Clinical Sciences, The Ohio State University, 601 Vernon L. Tharp Street, Columbus, OH 43210, USA*

Received 19 October 2009; received in revised form 8 January 2010; accepted 21 January 2010

KEYWORDS
Cardiology;
Echocardiography;
Left ventricle;
Systolic time intervals;
Horse

Abstract *Objective:* To study the applicability of anatomical M-mode (AMM) for assessment of left ventricular (LV) size and function in horses, evaluate agreement with conventional M-mode (CMM), determine reliability, and establish reference intervals for AMM measurements.
Animals: 98 horses; 13.1 $\pm$ 5.6 years; 538 $\pm$ 78 kg.
Methods: Two-dimensional and M-mode recordings were analyzed retrospectively. Standard LV dimensions and indices of LV function, including time intervals, were measured in CMM and compared with AMM studies in long-axis (lx) and short-axis (sx) views.
Results: The percentages of measureable cycles were 99%, 97%, and 90% for routine LV studies in CMM_{sx}, AMM_{sx}, and AMM_{lx} mode. For time intervals, $\geq$ 93% of cycles could be measured using AMM compared to a maximum of 77% using CMM. AMM_{sx} measurements agreed well with CMM_{sx} measurements for LV studies; the agreement of AMM_{lx} with CMM_{sx} was markedly lower. The LV ejection time and the duration of electromechanical systole, but not the LV pre-ejection period and the index of myocardial performance, showed fair agreement between methods. Intraobserver and interobserver measurement variabilities were low for most variables.
Conclusions: AMM can replace CMM for assessment of LV dimensions in horses, but is not recommended for measurement of time intervals.

* Corresponding author.
E-mail address: cschwarzwald@vetclinics.uzh.ch (C.C. Schwarzwald).

1760-2734/$ - see front matter © 2010 Elsevier B.V. All rights reserved.
doi:10.1016/j.jvc.2010.01.002

Introduction

Echocardiography is a standard diagnostic procedure and an important part of clinical and experimental cardiac examinations in horses. Nevertheless, the echocardiographic assessment of left ventricular (LV) size and function is still a demanding challenge for veterinary cardiologists and is limited by a variety of technical, anatomical, and physiological issues. Conventional M-mode echocardiography (CMM) is widely used in current clinical practice for assessing LV size and function. Standard M-mode indices of LV size include the internal diameter of the LV cavity (LVID) and the thickness of the interventricular septum (IVS) and the LV free wall (LVPW), respectively. The LV fractional shortening (FS) and the LV internal diameter at peak systole, respectively, are the most commonly used M-mode-derived indices of LV systolic function. Other indices of LV function include systolic time intervals (pre-ejection period, PEP; ejection time, ET; and PEP/ET ratio) and the index of myocardial performance (IMP, also referred to as Tei-index).[1–6]

All of the above indices are routinely measured or calculated from M-mode recordings obtained from right parasternal short-axis views or occasionally from long-axis views.[1] The advantage of the CMM technique is the high pulse repetition frequency (200–1000 Hz), resulting in a high temporal resolution (1–5 msec) that allows accurate measurement of time intervals. The major limitation of CMM is that the cursor line can only be rotated around the apex of the imaging sector.[7] To achieve the exact orientation, CMM studies are typically guided by reference to a simultaneously obtained two-dimensional (2D) image. However, ideal alignment is not always possible because of individual thorax conformation, interference from lung or ribs, or a limited cardiothoracic window.[8] Furthermore, CMM does not allow tracking of valve motion during the cardiac cycle. Therefore, identification of onset and end of valve motion and measurement of time events by CMM is often difficult.

With advances in ultrasound technology such as high-frame rate 2D imaging, expanded digital cine memory, and powerful computer processing algorithms, it has become possible to develop a modified M-mode method that can overcome some of the limitations of CMM echocardiography.[8] The so called 'anatomical M-mode' (AMM)[c] can be applied directly during the echocardiographic examination ('live' AMM) or it can be used as a post-processing technique that creates M-mode studies from digitally stored 2D cine-loops. It allows the operator to position the M-mode cursor freely on the 2D image, independent of the sector apex. This technique also allows rendering M-mode studies from multiple orientations and updating the position of the M-mode cursor between measurements. Therefore, moving structures can be tracked during the cardiac cycle and identification of time events (i.e., valve opening and closure) is facilitated.[7,9] With AMM it is possible to reduce the duration of the echocardiographic examination, because AMM tracings can be derived offline from standard 2D recordings and can replace CMM studies that have to be conducted 'live'. The contras of AMM are related to the relatively low recording frame rate of 2D echocardiography (approximately 50 frames per second in horses), resulting in a relatively low temporal resolution (approximately 20 ms).[7–9] The ability to accurately and reliably measure time intervals on AMM recordings may therefore be limited.

The aim of this study was to investigate the applicability and the reliability of the AMM for assessment of LV size and function in horses and to evaluate the agreement of AMM with CMM measurements. We hypothesized that indices of LV size and function by AMM can be reliably obtained and are in good agreement with CMM indices. In addition, the study aimed at establishing reference intervals for indices of LV size and function measured with AMM in healthy horses.

Animals, materials and methods

Animals

The study population was chosen retrospectively and included horses that underwent an echocardiographic examination at The Ohio State University or at The University of Zurich between January 2005 and March 2009. Enrollment criteria were body weight $>$ 300 kg, age $>$ 2 years, and the availability of a complete, standardized echocardiogram of good quality, with an ECG recorded simultaneously and performed by a single operator (CCS) on a digital echocardiography system[d]. Ninety-eight horses (31 females, 67 geldings) with an age of 13.1 $\pm$ 5.6 years (n = 97) and a body weight of 538 $\pm$ 78 kg (n = 87) fulfilled the

[c] EchoPAC Software v6.1.2, GE Medical Systems, Milwaukee, WI.

[d] GE Vivid 7 ultrasound system, GE Medical Systems, Milwaukee, WI.

inclusion criteria. The study population included 49 Warmblood horses, 20 Standardbreds, 13 Thoroughbreds, 6 Arabians, 2 Icelandic horses, 2 Quarter horses, and 1 each of the following breeds: Haflinger, Freiberger, Paint, Cob, and Paso Fino; in 1 horse breed was not reported. All animals received adequate human care and were treated during the examination according to the ethical guidelines of the universities.

Of these horses, 78 were in normal sinus rhythm (NSR) and 20 were in atrial fibrillation (AF). In the NSR group, 42 horses had a structurally and functionally normal heart. The remaining 36 horses had structural or functional abnormalities as detected by echocardiography. Grading of severity of valvular regurgitation was achieved using a scoring system based on the duration of the regurgitant signal, high-velocity jet area and flow disturbance, regurgitant signal duration, and the number of imaging planes in which the high-velocity jet could be observed in the receiving chamber.[10] The following abnormalities were diagnosed: Mild mitral regurgitation (MR) ($n = 6$), moderate MR ($n = 6$), severe MR ($n = 2$), mild aortic regurgitation (AR) ($n = 4$), moderate AR ($n = 3$), severe AR ($n = 2$), moderate tricuspid regurgitation (TR) ($n = 1$), mild MR & mild AR ($n = 2$), mild MR & moderate AR ($n = 2$), mild MR & severe AR ($n = 1$), moderate MR & mild AR ($n = 1$), moderate MR & severe AR ($n = 1$), moderate MR & moderate TR ($n = 1$), mild AR & mild pulmonic regurgitation (PR) ($n = 2$), congestive heart failure with moderate MR & severe AR & moderate-to-severe TR & mild PR ($n = 1$), and congestive heart failure due to myocarditis ($n = 1$).

In the AF group, 5 horses had a structurally normal heart as determined by echocardiography. The remaining 15 horses had one of the following diagnoses: Mild MR ($n = 1$), mild AR ($n = 1$), mild TR ($n = 2$), mild PR ($n = 2$), mild MR & moderate AR ($n = 1$), severe MR & severe AR ($n = 1$), moderate MR & mild PR ($n = 1$), mild MR & mild TR ($n = 1$), moderate MR & mild TR ($n = 1$), mild AR & mild PR ($n = 1$), mild AR & mild TR ($n = 2$), moderate MR & moderate AR & moderate TR ($n = 1$). Two of these horses had signs of pulmonary hypertension (maximum velocity of the tricuspid regurgitation jet measured by spectral Doppler exceeded 3.5 m/s) and 1 horse was in congestive heart failure.

Echocardiography

All horses underwent a complete echocardiographic examination performed by a single operator (CCS) according to a standardized protocol. During the examination, all horses were standing in a quiet room and restrained by an experienced handler. Three horses were sedated with 4 mg of detomidine[e] intravenously prior to the examination, while the remaining 95 horses were not sedated during the examination. Transthoracic 2D echocardiography and 2D-guided CMM echocardiography were performed using a high-end digital echocardiograph[d] with a phased array sector transducer[f] working at frequencies from 1.5/3.1 to 1.9/4.0 MHz (octave harmonics). The median frame rate for the 2D cine-loop recordings was 53.9 frames/s (fps), with a range of 28.9–71.1 fps. Twenty-five echocardiograms were recorded at frame rates below 50 fps. An ECG was recorded simultaneously for timing of measurements within the cardiac cycle.

All recordings were preformed in standard right-parasternal imaging planes.[1] The LV was imaged in a long-axis (four-chamber) view in 2D mode and in a short-axis view at the chordal level in 2D mode and CMM. The mitral valve (MV) was imaged in a four-chamber view in 2D mode and in a short-axis view in 2D mode and CMM. The aortic valve (AoV) was imaged in a long-axis view of the left ventricular outflow tract (LVOT) in 2D mode and in a short-axis view at the level of the valve in CMM.

In each imaging plane, at least 3 representative, non-consecutive cardiac cycles were recorded in horses with NSR and at least 5 cycles were recorded in horses with AF. All images were stored either as CMM still images or as 2D cine-loops in digital raw-data format.

Anatomical M-mode analyses

All AMM analyses were performed offline by a single observer (PAG) using the analysis software of the echocardiography system[c]. The AMM tracings of the LV, the MV, and the AoV were generated by positioning the electronic cursor through the respective 2D cine-loop recordings. In LV short-axis view, the AMM cursor was positioned through the lumen of the LV, bisecting the interventricular septum, the LV cavity, and the LV free wall into two equal parts throughout the cardiac cycle (Fig. 1). In LV long-axis view, the AMM cursor was positioned at the chordal level, parallel to the MV annulus (online-only Data Supplement Fig. I). For analysis of MV motion, the AMM cursor was placed across the MV leaflets in both the long-axis recordings (parallel to the MV annulus) (Online-only Data Supplement Fig. II) and in the short-axis

[e] Detomidine (Domosedan®), Pfizer AG, Berlin, Germany.
[f] M3S and M4S phased array transducer, GE Medical Systems, Milwaukee, WI.

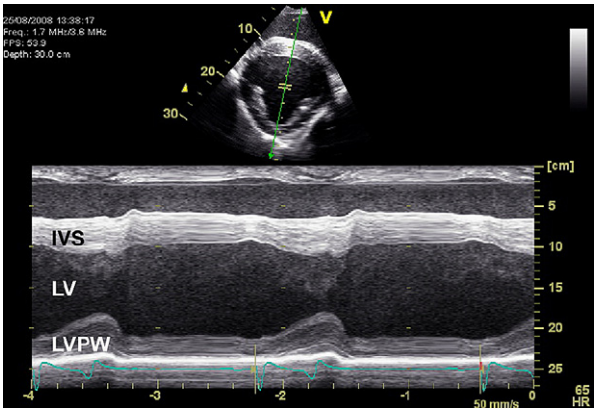

Figure 1 Anatomical M-mode image of the left ventricle (LV), reconstructed from a digitally stored 2D cine-loop recording obtained from a right parasternal short-axis view at the chordal level. The AMM cursor line (green) is positioned through the lumen of the LV, bisecting the interventricular septum (IVS), the LV cavity, and the LV free wall (LVPW) into two equal parts throughout the cardiac cycle. An ECG is superimposed for timing (For interpretation of the references to colour in this figure legend, the reader is referred to the web version of this article).

recordings of the valve (Fig. 2). For analysis of AoV motion, the AMM cursor was placed across the AoV leaflets (parallel to the AoV annulus) in the long-axis recordings of the valve (Fig. 3). For correct identification of MV and AoV opening and closure,

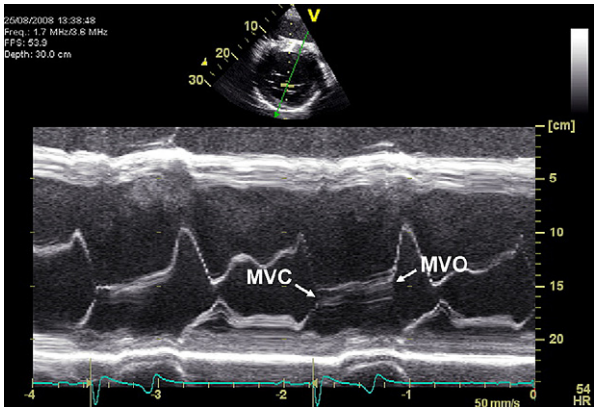

Figure 2 Anatomical M-mode image of mitral valve motion, reconstructed from a digitally stored 2D cine-loop recording obtained from a right parasternal short-axis view at the level of the mitral valve. The AMM cursor line (green) is placed across the MV leaflets. Notice that in this example, both the time of mitral valve closure (MVC) and the time of mitral valve opening (MVO) can be identified on the same AMM tracing (For interpretation of the references to colour in this figure legend, the reader is referred to the web version of this article).

respectively, the AMM cursor was moved to follow the valve leaflets during the cardiac cycle until the opening and closure events were clearly delineated. Where these time events were not clearly visible using a single cursor position, two different cursor positions were used at end-systole (AoV closure, MV opening) and end-diastole (AoV opening, MV closure). Anatomical M-mode was not applied to short-axis recordings of the AoV, because the available cine-loop recordings of the AoV and the left atrium (LA) in short-axis had been optimized for measurement of the LA but not for assessment of AoV motion, and because preceding pilot studies had shown that derived AMM tracings rarely allowed proper identification of both AoV opening and closure.

Measurements

All measurements were performed offline by a single observer (PAG) using the digital raw-data image files. The measurements were performed on both the CMM and the AMM tracings. In horses with NSR, we attempted to analyze 3 non-consecutive, randomly chosen cardiac cycles for each imaging plane and echocardiographic modality. Cycles immediately following an incident of 2nd degree atrio-ventricular block were excluded from analyses. In horses with AF, we attempted to analyze 5 consecutive cycles, independent of the length of the cycle. In horses, in which the available recordings did not contain a sufficient number of complete cardiac cycles for all imaging planes, all available cycles were measured. On some recordings, unambiguous identification of anatomical landmarks for measurements was not possible on all cycles. In those cases, we measured only the cycles, in which the landmarks could be clearly identified. For each variable, the number of available cycles and the number of measurable cycles were noted. The heart rate (HR) of each measured cycle was calculated based on the RR interval preceding the analyzed cycle ($HR = 60{,}000/RR$).

For LV analyses, the 'trailing-inner-inner-leading' edge method was used. End-diastolic measurements of LV dimensions were timed to the peak of the electrocardiographic R wave, because the onset of the R wave was not always clearly visible and the Q wave was usually absent in the lead used. End-systolic measurements of LV dimensions were made at the point of maximal excursion of the interventricular septum and the LV free wall. The following dimensions were measured on the LV tracings: The interventricular

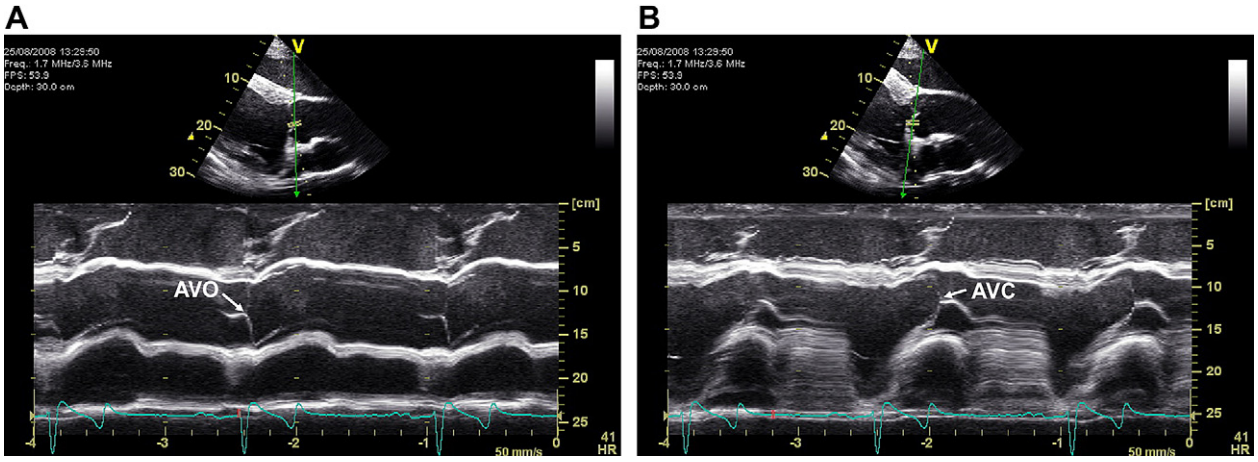

Figure 3 Anatomical M-mode images of aortic valve motion, reconstructed from a digitally stored 2D cine-loop recording obtained from a right parasternal long-axis view of the left ventricular outflow tract. The AMM cursor line is placed across the AoV leaflets, parallel to the AoV annulus. Depending on the position of the cursor line, the time of aortic valve opening (Fig. 3A, AVO) or aortic valve closure (Fig. 3B, AVC) can be identified. The ability to track aortic valve motion by AMM greatly facilitates measuring the systolic time intervals compared to CMM imaging.

septal thickness at end-diastole (IVSd) and at peak systole (IVSs), the LV internal diameter at end-diastole (LVIDd) and at peak systole (LVIDs), and the LV free wall thickness at end-diastole (LVPWd) and at peak systole (LVPWs). The LV fractional shortening (FS, in %) was calculated as FS = (LVIDd−LVIDs)/LVIDd × 100. The LV mass (in g) was calculated as LV mass = 1.04 × [(LVIDd + LVPWd + IVSd)^3−LVIDd^3]−13.6.[11–13] The relative LV wall thickness at end-diastole (RWT) was calculated as RWT = (LVPWd + IVSd)/LVIDd. The mean LV wall thickness at end-diastole (MWT) was calculated as MWT = (LVPWd + IVSd)/2.

On the MV tracings, the MV closure-to-opening interval (MVCO) was measured as the time interval from MV closure to MV opening (Fig. II) (Fig. 2).

On the AoV tracings, the LV pre-ejection period (LVPEP) was measured as the time interval from the peak of the echocardiographic R wave to the opening of the AoV on the AoV tracing, and LV ejection time (LVET) was measured as the time interval from opening to closure of the AoV on the same tracing (Fig. 3). The LVPEP/LVET ratio and the duration of electromechanical systole (EMS = LVPEP + LVET) were calculated.

For each measured variable, the average of the realized measurements was calculated and used for further analyses. With the averaged data, the following compound indices (i.e., indices calculated from measurements made in different imaging planes and in different cardiac cycles) were calculated: The mean velocity of circumferential fiber shortening, Vcf = (LVIDd−LVIDs)/(LVIDd × LVET); the rate-corrected mean velocity of circumferential fiber shortening, Vcfc = (LVIDd−LVIDs)/(LVIDd × (LVET/√RR)); and the index of myocardial performance (Tei-Index), IMP = (MVCO−LVET)/LVET.

Measurement reliability

To determine the intraobserver and interobserver measurement reliability, a subgroup of 5 randomly selected horses was re-analyzed by the same observer (PAG) and by a second observer (CCS). The second analyses also included repeated generation of AMM tracings from 2D cine-loops. Both observers were blinded to signalment, diagnosis, previously measured cycles, and previous measurements.

Data analysis and statistics

Graphical presentation, data analyses, and statistics were performed using commercial computer software[g,h,i]. For each variable and each echocardiographic modality (i.e., CMM, AMM), the percent ratio of measurable over available cardiac cycles was calculated. For analysis of agreement between CMM and AMM, measurements were only included if the average HR differed by less than 25%. Data points for which HR differed by > 25% between CMM and AMM were excluded from analysis, in order to reduce bias related to differences in heart rate rather than differences in

[g] Microsoft Office Excel 2008, Microsoft Corporation, Redmond, WA.
[h] GraphPad Prism v5.02 for Windows, GraphPad Software, San Diego, CA.
[i] SigmaStat v3.5, SPSS Inc, Chicago, IL.

echocardiographic modality. After averaging the realized measurements (i.e., 3 measurements for horses in NSR and 5 measurements for horses in AF), method agreement was assessed using Bland-Altman analyses. For each variable, mean bias and 95% limits of agreement were calculated and reported as absolute values and as percent values. The methodical details of Bland-Altman analyses have been described elsewhere.[14,15] Briefly, mean bias is calculated as the mean difference between the two methods and describes the average discrepancy of measurements obtained using the two methods. The 95% limits of agreement are calculated as the mean bias plus or minus 1.96 times the standard deviation of the differences between the two methods. For any variable, the difference between measurements using the two methods will lie within the limits of agreement in 95% of the time. Hence, bias and limits of agreement are indices of comparability between two methods that have to be interpreted in relation to the magnitude of the respective variable. Therefore, summary statistics (mean $\pm$ SD) for each variable were reported for comparison. Agreement was further assessed using Lin's concordance correlation.[16] Lin's concordance was reported as the sample concordance correlation coefficient (ρ_c) and its lower one-sided 95% confidence limit.[17,18] The coefficient ranges from 0 to 1 and increases in value as a function of the nearness of the data to the line of perfect concordance and the tightness of the data about this axis. To our knowledge, there is as yet no established descriptive scale for the degree of agreement of echocardiographic variables using ρ_c. Accordingly, ρ_c was regarded as a complementary measure of agreement that was used for comparison of the different variables and echocardiographic modalities within this study rather than as an absolute measure of agreement.

To establish reference intervals for the measured and calculated variables, we used the data from anamnestically and clinically healthy horses that were in normal sinus rhythm and had a structurally normal heart on echocardiographic examination. The healthy population was classified by breed into three groups: Warmbloods, Standardbreds and Thoroughbreds. For each group, reference intervals of each variable were reported with the 2.5% percentile being the lower limit and the 97.5% percentile being the upper limit of the interval. Body weight was reported as mean $\pm$ SD.

Intraobserver measurement reliability and interobserver measurement reliability were quantified by the within-subject variance for repeated measurements (residual mean square) determined by 1-way analysis of variance with the horses as groups.[19] The within-subject standard deviation (s_w) was calculated as the square root of the residual mean square. Measurement variability was reported in 2 ways: (1) The within-subject coefficient of variation (CV) expressed as a percent value was calculated as CV $= s_w/\text{mean} \times 100$ in order to compare the reliability of the various variables in this study.[19] The degree of variability was arbitrarily defined as follows: CV $< 5\%$, very low variability; 5–15%, low variability; 16–25%, moderate variability; >25%, high variability. (2) In addition to the CV, the absolute value below which the difference between 2 measurements will lie with 95% probability was estimated following the British Standards Institution (BSI) recommendations: BSI $= 1.96 \times \sqrt{2} \times s_w = 2.77 \times s_w$.[19] The BSI was reported to provide a clinically applicable measure of variability, hence an absolute value that allows comparison with measured changes in echocardiographic variables on a case-by-case basis.

Results

Table 1 summarizes the number of available cardiac cycles and the number of measurable cycles in the study population. The results show that the percentage of measureable cycles was comparable for LV studies performed in CMM in short-axis views (CMM_{sx}) and AMM in short-axis views (AMM_{sx}), and slightly lower for AMM in long-axis views (AMM_{lx}). For MV and AoV time intervals, the percentage of measurable cycles was markedly higher using AMM compared to CMM.

The results of the analyses of agreement are summarized in Table A (online-only Data Supplement). Generally, for the LV study, AMM_{sx} measurements agreed well with CMM_{sx} measurements, while the agreement of AMM_{lx} measurements was markedly lower, particularly for the septal thickness, the

Table 1 Ratio of measurable cardiac cycles over available cardiac cycles for conventional M-mode applied to short-axis imaging planes (CMM_{sx}) and anatomical M-mode applied to short-axis (AMM_{sx}) and long-axis (AMM_{lx}) imaging planes.

	LV study	MVCO	LVPEP, LVET
CMM_{sx}	309/312 (99%)	237/307 (77%)	160/306 (52%)
AMM_{sx}	255/263 (97%)	224/229 (98%)	–
AMM_{lx}	264/295 (90%)	285/299 (95%)	268/287 (93%)

LV study: Measurements of left ventricular dimensions (see Table 2). MVCO: Mitral valve closure-to-opening interval. LVPEP: Left ventricular pre-ejection period. LVET: Left ventricular ejection time.

Table 2 Reference intervals for CMM and AMM measurements in clinically healthy horses in normal sinus rhythm, reported as the interval between the 2.5% and the 97.5% percentile.

	Breed	CMM_{sx}			AMM_{sx}			AMM_{lx}		
		Warmbloods	Standardbreds	Thoroughbreds	Warmbloods	Standardbreds	Thoroughbreds	Warmbloods	Standardbreds	Thoroughbreds
	BWT(kg)	550 ± 59	539 ± 31	548 ± 59	550 ± 59	539 ± 31	548 ± 59	550 ± 59	539 ± 31	548 ± 59
LV	HR (/min)	32–66	28–49	29–55	30–67	32–48	30–50	34–68	29–51	31–47
		($n = 13$)	($n = 15$)	($n = 7$)	($n = 13$)	($n = 9$)	($n = 4$)	($n = 11$)	($n = 9$)	($n = 5$)
	IVSd (cm)	2.7–3.8	2.5–3.8	3.0–3.7	2.7–3.5	2.9–3.5	2.9–3.8	2.1–3.0	1.8–3.0	2.0–3.2
		($n = 13$)	($n = 15$)	($n = 7$)	($n = 13$)	($n = 9$)	($n = 4$)	($n = 11$)	($n = 9$)	($n = 5$)
	LVIDd (cm)	9.9–12.9	10.2–13.2	10.9–13.6	10.1–13.3	10.0–13.7	10.9–12.9	10.7–12.6	11.0–14.3	11.6–12.6
		($n = 13$)	($n = 15$)	($n = 7$)	($n = 13$)	($n = 9$)	($n = 4$)	($n = 11$)	($n = 9$)	($n = 5$)
	LVPWd (cm)	1.9–2.9	1.7–3.1	2.2–2.7	1.8–3.2	1.7–2.9	2.3–2.9	1.9–2.5	1.8–3.6	2.0–2.6
		($n = 13$)	($n = 15$)	($n = 7$)	($n = 13$)	($n = 9$)	($n = 4$)	($n = 11$)	($n = 9$)	($n = 5$)
	IVSs (cm)	4.5–5.2	3.8–5.5	4–5.2	4.1–5.4	4.2–5.6	4.1–5.2	3.7–4.4	2.8–4.5	3.4–4.4
		($n = 13$)	($n = 15$)	($n = 7$)	($n = 13$)	($n = 9$)	($n = 4$)	($n = 11$)	($n = 9$)	($n = 5$)
	LVIDs (cm)	5.5–8.3	5.3–8.9	6.6–8.7	5.9–8.8	5.0–9.0	6.7–9.4	5.7–8.6	5.6–8.8	6.4–8.3
		($n = 13$)	($n = 15$)	($n = 7$)	($n = 13$)	($n = 9$)	($n = 4$)	($n = 11$)	($n = 9$)	($n = 5$)
	LVPWs (cm)	3.5–4.9	2.7–4.3	3.9–4.7	3.0–5.1	2.7–4.6	4–4.6	3.2–4.3	3.2–4.8	4.0–4.7
		($n = 13$)	($n = 15$)	($n = 7$)	($n = 13$)	($n = 9$)	($n = 4$)	($n = 11$)	($n = 9$)	($n = 5$)
	LV FS (%)	33–46	31–49	32–42	32–49	33–50	32–42	30–52	25–51	34–45
		($n = 13$)	($n = 15$)	($n = 7$)	($n = 13$)	($n = 9$)	($n = 4$)	($n = 11$)	($n = 9$)	($n = 5$)
	LV mass (g)	2482–4649	2100–5477	3262–4733	2598–5550	2410–5040	2197–5876	2253–3725	1890–4368	2594–3897
		($n = 13$)	($n = 15$)	($n = 7$)	($n = 13$)	($n = 9$)	($n = 4$)	($n = 11$)	($n = 9$)	($n = 5$)
	MWT (cm)	2.4–3.2	2.2–3.5	2.7–3.2	2.4–3.2	2.4–3.2	2.6–3.4	2.0–2.6	1.9–3.2	2.1–2.7
		($n = 13$)	($n = 15$)	($n = 7$)	($n = 13$)	($n = 9$)	($n = 4$)	($n = 11$)	($n = 9$)	($n = 5$)
	RWT	0.41–0.63	0.39–0.56	0.40–0.56	0.38–0.61	0.38–0.57	0.41–0.62	0.33–0.47	0.32–0.54	0.36–0.43
		($n = 13$)	($n = 15$)	($n = 7$)	($n = 13$)	($n = 9$)	($n = 4$)	($n = 11$)	($n = 9$)	($n = 5$)
	Vcf (circ/s)	0.66–1.03	0.57–0.90	0.64–0.86	0.70–1.03	0.73–1.07	0.79–0.83	0.67–1.13	0.62–1.18	0.78–1.04
		($n = 8$)	($n = 5$)	($n = 4$)	($n = 12$)	($n = 8$)	($n = 2$)	($n = 11$)	($n = 8$)	($n = 4$)
	Vcfc (circ/s)	0.83–1.19	0.75–1.04	0.84–1.14	0.88–1.31	0.92–1.30	0.98–1.03	0.88–1.26	0.68–1.40	0.96–1.33
		($n = 8$)	($n = 5$)	($n = 4$)	($n = 12$)	($n = 8$)	($n = 2$)	($n = 11$)	($n = 8$)	($n = 4$)
MV	HR (/min)	36–70	28–52	30–73	35–67	32–47	33–37	34–67	29–51	32–46
		($n = 12$)	($n = 11$)	($n = 6$)	($n = 12$)	($n = 5$)	($n = 3$)	($n = 12$)	($n = 10$)	($n = 5$)
	MVCO (ms)	441–673	516–671	361–769	450–706	543–684	547–599	457–736	525–692	608–643
		($n = 12$)	($n = 11$)	($n = 6$)	($n = 12$)	($n = 5$)	($n = 3$)	($n = 12$)	($n = 10$)	($n = 5$)
	IMP	0.13–0.40	0.01–0.49	0.06–0.43	0.18–0.49	0.19–0.62	0.24–0.37	0.20–0.53	0.15–0.46	0.30–0.48
		($n = 6$)	($n = 4$)	($n = 3$)	($n = 11$)	($n = 5$)	($n = 2$)	($n = 12$)	($n = 7$)	($n = 4$)
AoV	HR (/min)	30–68	29–46	34–44				34–64	29–50	32–58
		($n = 8$)	($n = 4$)	($n = 4$)				($n = 13$)	($n = 12$)	($n = 6$)
	LVPEP (ms)	37–61	50–110	52–104				47–94	52–99	52–86
		($n = 8$)	($n = 4$)	($n = 4$)				($n = 13$)	($n = 11$)	($n = 6$)
	LVET (ms)	388–532	386–547	458–538				381–488	397–483	370–488
		($n = 8$)	($n = 4$)	($n = 4$)				($n = 13$)	($n = 11$)	($n = 6$)
	LVPEP/LVET	0.07–0.13	0.10–0.29	0.10–0.23				0.11–0.20	0.12–0.21	0.14–0.18
		($n = 8$)	($n = 4$)	($n = 4$)				($n = 13$)	($n = 11$)	($n = 6$)
	EMS (ms)	440–588	497–614	562–600				429–573	477–582	421–575
		($n = 8$)	($n = 4$)	($n = 4$)				($n = 13$)	($n = 11$)	($n = 6$)

BWT: Body weight (reported as mean ± SD). For remainder of the key see text.

free wall thickness, and the derived variables (i.e., LV mass, MWT, and RWT). Among the time intervals, MVCO, LVET and EMS showed fair agreement between CMM_{sx} and AMM measurements, while agreement of LVPEP was low. The calculated compound indices (i.e., Vcf, Vcfc, and IMP) showed markedly lower agreement than measured indices. Agreement of the IMP was poor.

The reference intervals for all echocardiographic variables for clinically healthy horses are summarized in Table 2, grouped by echocardiographic modality and breed.

Reliability data of all echocardiographic variables, grouped by echocardiographic modality, are summarized in Table B (online-only Data Supplement). Based on the CV, intraobserver measurement variability and interobserver measurement variability were very low to low for all variables, with the exception of the IMP, showing low to moderate variability. Overall, variability was lower for CMM_{sx} and AMM_{sx} compared to AMM_{lx}. Within each echocardiographic modality, interobserver measurement variability was generally slightly higher than intraobserver measurement variability, but they were not substantially different and were in a comparable range for all variables.

Discussion

The results of the current study indicate that AMM is readily applicable to analyze digitized 2D cine-loop recordings obtained from adult horses and that, for most instances, is reliable and in good agreement with routine CMM measurements of LV size and LV function.

The AMM technique offers several advantages over the CMM methodology. In clinical routine, the most useful features of AMM are the ability to generate AMM tracings offline, the free orientation of the cursor line, and the tracking capabilities.[7,9] The fact that AMM can be applied as a post-processing feature allows reducing the time required for acquiring echocardiographic recordings by several minutes. This may be of particular interest when examining animals that need to be physically restrained during the examination. The possibility to freely orientate the cursor line permits studying any cardiac structure upon every angle of interrogation. It allows anatomically consistent placement of the cursor line, resulting in better standardization of the examination and a higher degree of accuracy and precision.[8] The tracking function allows to follow moving structures (e.g., valve leaflets) during cardiac cycle to optimize and standardize cursor placement. Accordingly, we were able to show that the AMM method facilitates the measurement of MV and AoV time intervals, with a higher percentage of measureable cycles using the AMM technique. For the LV study, the tracking feature is less critical and therefore was not used in this study. Nonetheless, the percentage of measureable cycles was only slightly lower for AMM compared to CMM.

The quality of the stored 2D cine-loops of LV short-axis planes in this study allowed generating high-quality AMM_{sx} tracings. For routine LV measurements, the agreement of AMM_{sx} with CMM_{sx} and the measurement reliability were considered sufficiently high for use of AMM in clinical applications.

For LV measurements in AMM_{lx}, the percentage of measurable cycles, the agreement with CMM_{sx} measurements, and the measurement reliability were lower than observed in AMM_{sx}. This can be explained by a variety of methodological and technical issues. In some recordings, generation of AMM_{lx} tracings of the LV was hampered by inadequate image quality of the stored 2D cine-loops, in which the LV free wall could not be clearly identified. Another difficulty in AMM_{lx} tracings was the covering of the IVS by the tricuspid valve leaflet, impairing the ability to clearly identify the right-ventricular surface of the IVS. Because no measurements were taken from cycles where the anatomical landmarks (i.e., the endocardial and epicardial linings) could not be clearly identified, this resulted in a slightly lower percentage of measurable cycles in AMM_{lx} compared to AMM_{sx} or CMM_{sx} recordings.

Unlike AMM_{sx} tracings, AMM_{lx} tracings are obtained in an imaging plane that differs from the plane used for CMM_{sx} recordings. Therefore, although the same anatomical structures are studied in AMM_{sx} and AMM_{lx}, placement of the cursor line and the resulting measurements will inevitably be different. In both short-axis and long-axis imaging planes, translational motion of the heart causes changes of the position of the cursor line relative to the LV cavity, adds to measurement error, and decreases method agreement. Consistent placement of the AMM cursor in a LV long-axis view, at the chordal level, parallel to the mitral valve annulus, and without excessive interaction of the mitral valve leaflets, is hindered by the base-to-apex shortening effect of the LV during the cardiac cycle. Furthermore, translational motion of the heart can also result in changing orientation of the imaging plane during the cardiac cycle, so that it does not always cross the LV at its maximum dimension. Obviously, translational motion and base-to-apex shortening effect are also present when recording 2D or CMM images in short-axis planes. However, they are less obvious to the

observer and may affect measurements to a lesser degree, as long as the cursor line crosses the LV at its widest dimension throughout the cardiac cycle. The detailed investigation of the influence of translational motion and base-to-apex LV shortening on the accuracy of AMM measurements was beyond the scope of this study.

The results indicate that AMM facilitates measurement of systolic time intervals by virtue of its tracking function. Tracking allows following the spatial position of the moving valves throughout the cardiac cycle, making it easier to identify the valve opening and the valve closure on the AMM tracing. Conversely, CMM does not allow tracking of moving structures and often does not depict time events clear enough to allow accurate and reliable measurement of time intervals. In this study, MVCO, LVET, and EMS by AMM could be measured reliably in over 90% of the cycles and showed fair agreement with CMM_{sx} measurements. The reliability and agreement with CMM of LVPEP and LVPEP/LVET by AMM were markedly lower, most likely because of the relatively short duration of the LVPEP, rendering it more susceptible to measurement errors and influence of low temporal resolution (see below). Therefore, the clinical use of LVPEP and LVPEP/LVET by AMM analysis of aortic valve motion is not recommended in horses.

Measurement of MVCO is primarily useful for calculation of the IMP, which is an index of combined systolic and diastolic myocardial performance. However, mitral valve motion is not only determined by LV myocardial function, but is also influenced by LV end-diastolic pressure, aortic insufficiency, and duration of the PQ interval, resulting in premature or delayed mitral valve closure.[20] This may result in difficulties measuring the MVCO and may indirectly impair the accuracy of the IMP to represent myocardial performance. Another problem when calculating the IMP using M-mode measurements of MVCO and LVET is the fact that time intervals are measured sequentially in different imaging planes and in different cardiac cycles. Consequently, the accuracy of the results may be compromised by fluctuations in HR.[5] To minimize the effect of HR in this study, the difference in HR between AMM and CMM measurements had to be less than 25%. Nonetheless, the IMP by AMM showed inferior agreement with CMM compared to other measurements and was characterized by only moderate reliability. Therefore, we suggest that derivation of the IMP from CMM or AMM tracings should not be recommended in horses.

Measurement variability is relevant to the study of method agreement because the measurement errors inherent to the two methods being compared limit the degree of agreement which is possible.[14] If one or both methods have high measurement variability, the agreement between the two methods will be poor as well. Hence, comparison of the 95% limits of agreement obtained from Bland-Altman analyses with the BSI value obtained from variability analyses provides additional information on the influences of measurement error on method agreement. Generally, the higher the BSI value is, the larger the influence of measurement error on method agreement will be. Overall, for LV measurements, variability was low and method agreement was high. Conversely, the measurement variability was higher, and the method agreement lower, for LVPEP, LEPEP/LVET, and IMP. For most instances, the interobserver variability was only slightly higher than the intraobserver variability, indicating that the AMM method is relatively robust to observer-related measurement errors.

The retrospective design of the study needs to be listed as one of its limitations. However, the fact that in both hospital locations one single operator performed all echocardiographic recordings following a standardized protocol and using the same type of digital ultrasound equipment certainly minimized the error introduced due to different recording techniques.

AMM studies are derived from 2D cine-loops and therefore are affected by the limitations of 2D echocardiography, namely lower resolution and frame rates. The CMM studies benefit from high pulse repetition frequency available for interrogation. The pulse repetition frequency provides a high degree of temporal and axial resolution that is ideal for study of mobile cardiac structures. In this study, 25 echocardiograms were recorded at frame rates below 50 fps, resulting in low temporal resolution (i.e., $>$20 ms). This may particularly have influenced agreement and reliability of the short-lasting LVPEP and the related LVPEP/LVET ratio. However, the majority of studies were recorded at frame rates above 50 fps. Furthermore, 3 to 5 measurements were averaged for each cycle, likely removing some of the effects of measurement error due to low temporal resolution. Nonetheless, as discussed above, the results of this study suggest that AMM may not be suitable for measurement of short-lasting time events in horses.

Another limitation concerns the reference intervals reported in this study. Reference intervals were reported for all variables, even for those where the number of available horses was very low. However, reference intervals should ideally be determined on populations larger than 50 to 100 individuals.[21] Therefore, the intervals reported

here must be interpreted with caution and should be regarded as preliminary.

Conclusion

The present study shows that AMM is applicable for assessment of LV size and function in horses. The results suggest that AMM_{sx} can replace CMM_{sx} for routine assessment of LV size and function, with generally high method agreement and adequate measurement reliability. However, it needs to be recognized that AMM measurements largely depend on the quality of the 2D cine-loop recordings that are used to generate the AMM tracings. Therefore, the availability of high-end digital echocardiography equipment is an important prerequisite to produce high-quality AMM tracings with adequately high frame rates. But even with appropriate equipment, accurate measurement of short-lasting time intervals is limited. Furthermore, M-mode measurements are limited to a single dimension, disregarding the fact that the heart is a complex three-dimensional structure. Recent human imaging guidelines emphasize the advantages of area-based and volume-based indices for assessment of chamber dilation and dysfunction, because linear measurements may be somewhat insensitive, particularly in the presence of non-uniform chamber enlargement, alterations in chamber geometry, and presence of regional wall motion abnormalities.[22] Therefore, one can argue that echocardiographic measurements should be made directly within the 2D recordings instead of using the derived AMM tracings. This would offer the advantage that two-dimensional area measurements and three-dimensional volume estimates could be obtained. In fact, the use of M-mode measurements may be regarded somewhat antiquated and is largely based on traditional conventions that were agreed on in times when the quality of 2D echocardiograms was still hampered by very low resolution and frame rates. However, M-mode measurements are still widely used for assessment of LV size and function in horses and may actually be superior to 2D cine-loop recordings for subjective visual assessment of LV wall motion patterns and LV systolic function. This study was not aimed at comparing the use of linear M-mode measurements with linear dimensions, area measurements, or volume estimates obtained from 2D echocardiograms. Therefore, further studies will be needed to show if M-mode measurements of LV size and function should still be considered state-of-the-art in the age of high-quality digital echocardiography.

The supplementary data associated with this article can be found in the on-line version at doi:10.1016/j.jvc.2010.01.002.

Conflict of interest

No conflict of interest.

References

1. Boon JA. The echocardiographic examination. In: Boon JA, editor. Manual of veterinary echocardiography. 1st ed. Baltimore: Williams & Wilkins; 1998. p. 35—150.
2. Lightowler C, Piccione G, Fazio F, Pidal G, Cattáneo ML. Systolic time intervals assessed by 2-D echocardiography and spectral Doppler in the horse. Anim Sci J 2003;74:505—510.
3. Tei C, Nishimura RA, Seward JB, Tajik AJ. Noninvasive Doppler-derived myocardial performance index: correlation with simultaneous measurements of cardiac catheterization measurements. J Am Soc Echocardiogr 1997;10:169—178.
4. Pellett AA, Tolar WG, Merwin DG, Kerut EK. The Tei index: Methodology and disease state values. Echocardiography 2004;21:669—672.
5. Tham EBC, Silverman NH. Measurement of the Tei index: a comparison of M-mode and pulse Doppler methods. J Am Soc Echocardiogr 2004;17:1259—1265.
6. Cui W, Roberson DA. Left ventricular Tei index in children: comparison of tissue Doppler imaging, pulsed wave Doppler, and M-mode echocardiography normal values. J Am Soc Echocardiogr 2006;19:1438—1445.
7. Carerj S, Micari A, Trono A, Giordano G, Cerrito M, Zito C, Luzza F, Coglitore S, Arrigo F, Oreto G. Anatomical M-mode: an old-new technique. Echocardiography 2003;20:357—361.
8. Oyama MA, Sisson DD. Assessment of cardiac chamber size using anatomic M-mode. Vet Radiol Ultrasound 2005;46:331—336.
9. Mele D, Pedini I, Alboni P, Levine RA. Anatomic M-mode: a new technique for quantitative assessment of left ventricular size and function. Am J Cardiol 1998;81:82G—85G.
10. Young LE, Rogers K, Wood JLN. Heart murmurs and valvular regurgitation in Thoroughbred racehorses: Epidemiology and associations with athletic performance. J Vet Intern Med 2008;22:418—426.
11. O'Callaghan MW. Comparison of echocardiographic and autopsy measurements of cardiac dimensions in the horse. Equine Vet J 1985;17:361—368.
12. Young LE, Rogers K, Wood JLN. Left ventricular size and systolic function in Thoroughbred racehorses and their relationships to race performance. J Appl Physiol 2005;99: 1278—1285.
13. Devereux RB, Reichek N. Echocardiographic determination of left-ventricular mass in man — anatomic validation of method. Circulation 1977;55:613—618.
14. Bland JM, Altman DG. Statistical-methods for assessing agreement between 2 methods of clinical measurement. Lancet 1986;1:307—310.
15. Bland JM, Altman DG. Measuring agreement in method comparison studies. Stat Methods Med Res 1999;8:135—160.
16. Lin's concordance correlation coefficient. Web-Calculator. Available at, http://www.niwa.cri.nz/services/free/statistical/concordance [accessed October 2009].

17. Lin LI. A concordance correlation coefficient to evaluate reproducibility. Biometrics 1989;45:255—268.
18. Lin LI. Correction: criteria for the validation of surrogate endpoints in randomized experiments. Biometrics 2000;56:324.
19. Bland M. Clinical measurement. In: Bland M, editor. An introduction to medical statistics. 3rd ed. Oxford: Oxford University Press; 2000. p. 268—293.
20. Boon JA. Evaluation of size, function, and hemodynamics. In: Boon JA, editor. Manual of veterinary echocardiography. 1st ed. Baltimore: Williams & Wilkins; 1998. p. 151—260.
21. Altman DG. Some common problems in medical research. In: Altman DG, editor. Practical statistics for medical research. Boca Raton: Chapman & Hall; 1991. p. 396—439.
22. Lang RM, Bierig M, Devereux RB, Flachskampf FA, Foster E, Pellikka PA, Picard MH, Roman MJ, Seward J, Shanewise J. Recommendations for chamber quantification. Eur J Echocardiogr 2006;7:79—108.

Online Supplement

Table A: Analysis of agreement between CMM and AMM measurements.

		CMM_{sx}	AMM_{sx}							AMM_{lx}						
				Bland-Altman Analysis				Lin`s Concordance Coefficient			Bland-Altman Analysis				Lin`s Concordance Coefficient	
	Variable	Mean ± SD	Mean ± SD	Bias (absolute)	95% LA (absolute)	Bias (%)	95% LA (%)	ρc	Lower 95% CL	Mean ± SD	Bias (absolute)	95% LA (absolute)	Bias (%)	95% LA (%)	ρc	Lower 95% CL
LV	HR (/min)	41 ± 10	41 ± 11	- 0.1	- 6.4 to 6.1	- 0.3	- 14.9 to 14.3	0.96	0.94	42 ± 10	0.7	- 10.0 to 11.5	1.7	- 23.2 to 26.7	0.85	0.80
	IVSd (cm)	3.1 ± 0.4	3.1 ± 0.4	- 0.04	- 0.54 to 0.45	- 1.3	- 17.3 to 14.6	0.81	0.74	2.4 ± 0.4	- 0.72	- 1.62 to 0.19	- 26.1	- 58.5 to 6.4	0.14	0.06
	LVIDd (cm)	12.0 ± 1.5	12.0 ± 1.6	0.03	- 0.94 to 0.99	0.3	- 7.9 to 8.4	0.95	0.93	12.1 ± 1.4	0.06	- 1.43 to 1.56	0.7	- 11.9 to 13.3	0.87	0.82
	LVPWd (cm)	2.5 ± 0.4	2.4 ± 0.4	- 0.05	- 0.68 to 0.58	- 2.3	- 28.3 to 23.6	0.71	0.62	2.3 ± 0.4	- 0.12	- 0.92 to 0.68	- 4.4	- 37.6 to 27.6	0.54	0.41
	IVSs (cm)	4.5 ± 0.5	4.6 ± 0.5	0.03	- 0.81 to 0.86	0.6	- 18.4 to 19.7	0.69	0.59	3.7 ± 0.8	- 0.81	- 2.34 to 0.71	- 20.8	- 55.5 to 13.9	0.20	0.10
	LVIDs (cm)	7.3 ± 1.1	7.3 ± 1.1	0.01	- 1.20 to 1.22	0.2	- 18.0 to 18.4	0.84	0.79	7.4 ± 1.3	0.04	- 1.78 to 1.86	0.1	- 25.0 to 25.2	0.72	0.62
	LVPWs (cm)	4.2 ± 0.6	4.2 ± 0.6	- 0.01	- 0.66 to 0.63	- 0.6	- 16.3 to 15.1	0.83	0.76	4.2 ± 0.6	- 0.18	- 1.26 to 0.91	- 4.8	- 35.5 to 26.0	0.57	0.45
	LV FS (%)	39 ± 6	39 ± 6	0.0	- 8.4 to 8.4	- 0.1	- 21.1 to 20.9	0.74	0.65	39 ± 6	0.3	- 13.7 to 14.4	0.9	- 36.0 to 37.9	0.36	0.19
	LV mass (g)	3938 ± 930	3857 ± 967	- 68.9	- 1033.0 to 895.1	- 2.0	- 27.8 to 23.7	0.86	0.81	3152 ± 790	-755.9	- 1805.0 to 293.0	- 21.4	- 49.5 to 6.9	0.59	0.50
	MWT (cm)	2.8 ± 0.3	2.8 ± 0.4	- 0.05	- 0.46 to 0.37	- 1.8	- 17.0 to 13.5	0.81	0.75	2.4 ± 0.3	- 0.42	- 1.01 to 0.17	- 16.3	- 39.0 to 6.4	0.36	0.26
	RWT	0.48 ± 0.10	0.47 ± 0.10	- 0.010	- 0.086 to 0.067	- 2.1	- 18.8 to 14.7	0.93	0.90	0.42 ± 0.10	- 0.060	- 0.221 to 0.102	- 13.7	- 47.8 to 20.6	0.56	0.45
	Vcf (circ/s)	0.85 ± 0.19	0.91 ± 0.18	0.052	- 0.188 to 0.293	6.2	- 19.7 to 32.1	0.75	0.64	0.92 ± 0.22	0.062	- 0.350 to 0.474	6.5	- 36.5 to 49.4	0.51	0.35
	Vcf_c (circ/s)	1.02 ± 0.17	1.11 ± 0.19	0.054	- 0.235 to 0.342	5.3	- 20.6 to 31.1	0.55	0.37	1.12 ± 0.20	0.067	- 0.383 to 0.517	6.2	- 35.5 to 47.9	0.28	0.07
MV	HR (/min)	42 ± 12	42 ± 13	- 0.4	- 8.2 to 7.5	- 0.5	- 18.0 to 17.1	0.92	0.89	43 ± 12	1.3	- 6.4 to 9.05	3.0	- 14.2 to 20.1	0.93	0.91
	MVCO (ms)	572 ± 78	595 ± 82	21.2	- 53.5 to 95.9	3.6	- 8.7 to 15.9	0.83	0.77	586 ± 81	18.7	- 63.6 to 101.1	3.2	- 10.9 to 17.4	0.81	0.74
	IMP	0.28 ± 0.17	0.36 ± 0.12	0.095	- 0.134 to 0.323	36.2	- 43.5 to 115.8	0.47	0.29	0.35 ± 0.12	0.090	- 0.155 to 0.336	39.4	- 59.8 to 138.7	0.53	0.37
AoV	HR (/min)	43 ± 12								42 ± 11	- 0.1	- 9.1 to 8.9	0.2	- 19.0 to 19.3	0.93	0.90
	LVPEP (ms)	74 ± 32								81 ± 28	12.7	- 22.0 to 47.3	19.0	- 27.6 to 65.6	0.77	0.68
	LVET (ms)	460 ± 61								437 ± 51	- 26.0	- 92.2 to 40.1	- 5.7	- 20.3 to 8.9	0.76	0.67
	LVPEP/LVET	0.17 ± 0.09								0.19 ± 0.09	0.039	- 0.056 to 0.134	24.6	- 27.9 to 77.1	0.80	0.72
	EMS (ms)	534 ± 55								517 ± 52	- 13.3	- 75.1 to 48.4	- 2.4	- 14.3 to 9.5	0.81	0.73

LV: Left ventricle. MV: Mitral valve. AoV: Aortic valve.
CMM_{sx}: Conventional M-mode short-axis. AMM_{sx}: Anatomical M-mode short-axis. AMM_{lx}: Anatomical M-mode long-axis.
SD: Standard deviation. LA: Limits of agreement. ρc: Concordance correlation coefficient. CL: Confidence limit.
HR: Heart Rate. IVSd: Interventricular septal thickness at end-diastole. LVIDd: Left ventricular internal diameter at end-diastole. LVPWd: Left ventricular free wall thickness at end-diastole. IVSs: Interventricular septal thickness at peak systole. LVIDs: Left ventricular internal diameter at peak systole. LVPWs: Left ventricular free wall thickness at peak systole. LV FS: Left ventricular fractional shortening. LV mass: Left ventricular mass. MWT: Mean left ventricular wall thickness at end-diastole. RWT: Relative left ventricular wall thickness at end-diastole. Vcf: Mean velocity of circumferential fiber shortening. Vcf_c: Rate-corrected mean velocity of circumferential fiber shortening. MVCO: Mitral valve closure-to-opening interval. IMP: Index of myocardial performance. LVPEP: Left ventricular pre-ejection period. LVET: Left ventricular ejection time. EMS: Duration of electromechanical systole.

Table B: Reliability of echocardiographic variables of LV size and function measured by CMM and AMM.

		CMM_{sx}				AMM_{sx}				AMM_{lx}			
		Intraobserver		Interobserver		Intraobserver		Interobserver		Intraobserver		Interobserver	
	Variable	CV%	BSI	CV%	BSI	CV%	BSI	CV%	BSI	CV%	BSI	CV%	BSI
LV	HR (/min)	1.3	1.3	0.8	0.8	1.9	1.9	1.9	1.9	0.8	0.8	2.9	2.9
	IVSd (cm)	1.9	0.18	2.3	0.22	1.0	0.10	1.6	0.15	9.3	0.70	14.5	1.16
	LVIDd (cm)	1.4	0.46	1.6	0.53	1.6	0.54	2.2	0.75	2.8	0.93	2.2	0.74
	LVPWd (cm)	3.1	0.24	7.6	0.59	3.1	0.23	6.1	0.46	8.4	0.63	4.9	0.35
	IVSs (cm)	2.1	0.29	5.3	0.73	3.9	0.53	4.8	0.64	6.4	0.68	4.0	0.43
	LVIDs (cm)	2.1	0.42	4.7	0.96	1.8	0.36	4.0	0.80	3.1	0.64	4.3	0.92
	LVPWs (cm)	2.0	0.26	1.6	0.21	2.6	0.35	1.2	0.16	5.9	0.75	3.7	0.47
	LV FS (%)	3.6	4.1	5.7	6.2	1.1	1.3	5.1	5.7	4.6	4.9	9.3	9.5
	LV mass (g)	2.5	418.1	4.5	778.7	2.5	406.0	4.4	736.1	6.5	919.1	9.0	1299.8
	MWT (cm)	1.3	0.11	4.0	0.34	1.1	0.09	2.8	0.23	6.4	0.49	7.7	0.59
	RWT	1.9	0.028	5.7	0.083	2.0	0.028	4.8	0.069	9.7	0.125	9.0	0.115
	Vcf (circ/s)	2.3	0.055	5.3	0.122	3.6	0.094	3.3	0.081	3.0	0.076	8.6	0.200
	Vcf_c (circ/s)	2.4	0.074	5.5	0.162	3.7	0.123	3.1	0.099	3.1	0.100	7.8	0.236
MV	HR (/min)	2.1	2.1	2.8	2.8	1.2	1.2	1.1	1.1	1.9	1.9	3.2	3.2
	MVCO (ms)	1.3	22.5	2.5	41.2	3.7	62.8	4.2	70.4	3.8	65.4	6.4	107
	IMP	11.3	0.079	16.9	0.124	12.6	0.135	16.7	0.168	22.6	0.243	24.7	0.249
AoV	HR (/min)	0.9	0.9	3.6	3.8					0.3	0.3	1.6	1.6
	LVPEP (ms)	7.9	14.9	11.0	18.7					10.8	24.1	11.7	25.5
	LVET (ms)	2.6	35.2	3.6	47.1					3.0	36.4	2.9	35.4
	LVPEP/LVET	6.5	0.026	12.6	0.046					13.0	0.066	14.3	0.071
	EMS (ms)	3.0	45.5	3.2	46.8					1.9	20.1	1.5	22.3

CV%: Coefficient of variation (%). BSI: Absolute value below which the difference between two measurements will lie with 95% probability (following the British Standards Institution). For remainder of the key see Table 2.

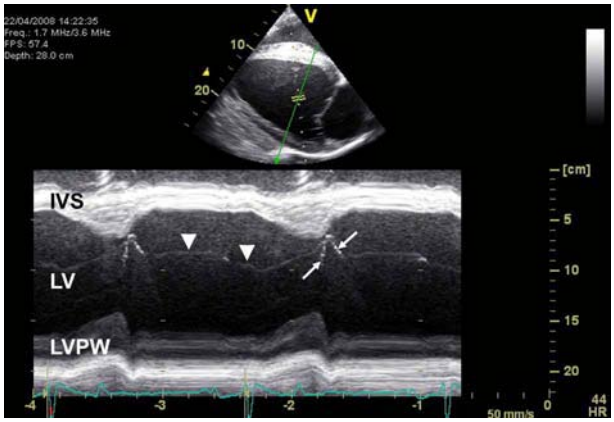

Figure I: Anatomical M-mode image of the left ventricle (LV), reconstructed from a digitally stored 2D cineloop recording obtained from a right parasternal long-axis view. Notice that the AMM cursor line (green) is positioned at the chordal level, parallel to the MV annulus and does not originate from the top of the 2D imaging sector. A chordal trace is visible within the LV lumen (arrowheads). The tip of the septal mitral valve leaflet appears in the LVlumen as it crosses the cursor line during early diastole (arrows). IVS, interventricular septum; LVPW, LV free wall.

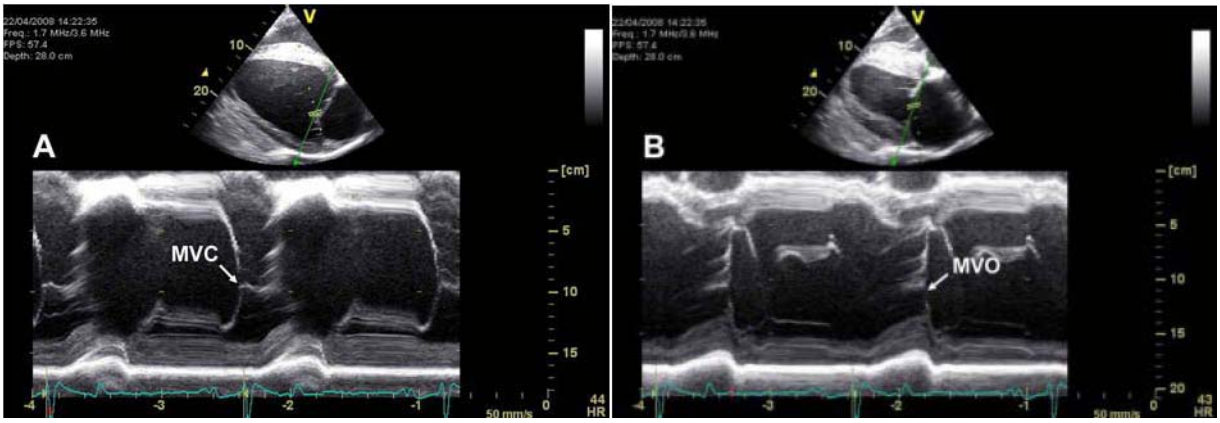

Figure II: Anatomical M-mode images of mitral valve motion, reconstructed from a digitally stored 2D cineloop recording obtained from a right parasternal long-axis view. The AMM cursor line (green) is placed across the MV leaflets. Depending on the position of the cursor line, the time of mitral valve closure (Figure IIA, MVC) or mitral valve opening (Figure IIB, MVO) can be identified. The ability to track mitral valve motion by AMM greatly facilitates measuring the mitral valve closure-to-opening time compared to conventional M-mode imaging.